Band Gap Engineering in Ni Doped ZnO Thin Films For use in Optoelectronic Devices

Santhosh.V. S
Department of Physics, M.G.College
Thiruvananthapuram, Kerala,India

K. Rajendra Babu
Department of Physics, M.G.College
Heera College of Engineering and Technology
Thiruvananthapuram,Kerala,India

Deepa. M
Department of Physics, All Saints' College
Thiruvananthapuram, Kerala, India

***Abstract* :- Pure and Ni doped ZnO thin films were deposited onto glass substrates by sol-gel spin coating method. Ni^{2+} / Zn^{2+} content in the starting solution was varied from 0 to 0.5 at%. Structural, compositional, morphological, optical, luminescence and electrical properties of the films were analyzed using X-ray diffraction (XRD), X-ray photoelectron spectroscopy (XPS), scanning electron microscopy (SEM), UV-vis spectroscopy, photoluminescence(PL) spectroscopy and four probe measurements respectively. All the films were preferentially oriented along the (002) plane and had a hexagonal wurtzite structure. Average crystallite size was found to increase with increase in Ni content. At higher Ni doping concentration of 0.4 and 0.5 at% the films were in a state of tensile stress. Significant changes in surface morphology were observed in the SEM images with increase in Ni content. Optical band gap was found to increase from 3.21 to 3.44 eV when Ni content in the films was varied from 0 to 0.5 at%. Porosity was found to decrease with increase in Ni content. Sharp UV emission was observed in the pure ZnO film. A blue shift in UV emission peak was observed upon Ni doping. Decrease in resistivity was observed with increase in Ni content which is correlated with increase in average crystallite size of the films.**

Keywords: ZnO thin films, sol-gel spin coating, stress, optical properties, porosity photoluminescence

I. INTRODUCTION

Zinc oxide (ZnO) is a II – VI direct wide band gap semiconductor with a free exciton binding energy of 60 meV [1]. It has a variety of applications in gas sensors, piezoelectric devices, solar cells, transparent electrodes, varistors, photodetectors, spintronic devices, surface acoustic wave devices etc. ZnO thin films exhibit high conductivity and optical transparency in the visible range, which makes it suitable for use in display devices. It is also widely used in optoelectronic devices such as laser diodes, UV diodes and light emitting diodes [2-5].

Doping ZnO with various elements is a widely employed technique to improve the structural, optical, electrical and magnetic properties of ZnO thin films. Transition metals such as Ni, Fe and Mn are attractive dopants for ZnO because they are isomorphic to Zn, possess variable oxidation states and have different acceptor properties in a ZnO matrix, thus affecting the electronic surface band structure of ZnO.

Ni is an important dopant that can increase the magnetic properties of ZnO thin films. Ni^{2+} has the same valency as that of Zn^{2+}. Also, its ionic radius (0.069 nm) is close to that of Zn^{2+} (0.074 nm). Hence Ni^{2+} can replace Zn^{2+} in ZnO lattice. There are various reports in literature as to how structural and optical properties of ZnO thin films vary when doped with Ni [6-9]. However, these studies do not show a consistent variation in the optical and photoluminescence properties of ZnO thin films when doped with Ni. Optical band gap was found to increase with increasing Ni content as reported by some authors [6,7]. But Pandey et al. has reported that optical band gap decreases when doped with Ni [8]. Only UV emission is observed in Ni doped ZnO thin films as reported by some authors [7,9]. But, Farag et al. has reported that UV emission is absent and that a very weak visible emission is observed in Ni doped ZnO thin films [6]. This variation in reports has motivated the authors to conduct the present work. The effect of Ni doping on the structural, optical, photoluminescence and electrical properties of ZnO thin films deposited by sol-gel technique is investigated in the present study.

Undoped and doped ZnO thin films can be prepared by various deposition techniques such as RF magnetron sputtering [10], Molecular beam epitaxy(MBE)[11], metal organic chemical vapor deposition(MOCVD) [12], pulsed laser deposition(PLD)[13] and the sol-gel process[14-16]. The present study analyses the structural, compositional, optical, and electrical characteristics of pure and Ni doped ZnO thin films by sol-gel method as this is an easy technique that can produce good quality films with high homogeneity. The method also offers better control of film composition.

II. EXPERIMENTAL

Pure and Ni doped ZnO thin films were deposited onto glass substrates by sol-gel spin coating method. 0.5 M ethanolic solution of zinc acetate, prepared by dissolving

0.05 mol of zinc acetate 2-hydrate ($Zn(OAC)_2$) ($Zn(CH_3COO)_2 .2H_2O$) (99.99%,Sigma Aldrich) in 100 ml of ethanol(99.99%,Sigma Aldrich) was used as the precursor sol. Diethanolamine (DEA) ($NH(CH_2CH_2OH)_2$) (99.99%,Sigma Aldrich) was added as stabilizer. DEA/$Zn(OAC)_2$ molar ratio was 1:1. Ni was added as dopant in the form of nickel chloride hexahydrate($NiCl_2.6H_2O$(99.99%, Sigma Aldrich). The mixture was stirred by a magnetic stirrer at 60 ^oC for 1 h, until a clear and homogeneous sol was formed. The atomic percentage of Ni $^{2+}$/Zn $^{2+}$ in the sol was 0, 0.1, 0.2, 0.3, 0.4 and 0.5 at%. Films were deposited after the sol was aged for 24 h.

Before film deposition, the glass substrates were cleaned with HCl and distilled water. Deposition was carried out at a spinning speed of 2000 rpm for 30 s. The films were then dried at 573 K for 2 min. on a hot plate. Since the boiling point of the dissolving solution and the thermal decomposition of zinc acetate is below 523 K, the pre heat treatment temperature is high enough to completely evaporate the organics from the crystalline ZnO films. The pure, 0.1, 0.2, 0.3, 0.4 and 0.5 at% Ni doped ZnO thin films were coded ZO, 0.1NZO, 0.2NZO, 0.3NZO, 0.4NZO and 0.5NZO respectively.

The crystal quality and phase analysis of the prepared samples were carried out using an X-ray diffractometer (Bruker D8 Advance). The electronic states of element were estimated by X-ray photoelectron spectroscopy (XPS, KRATOS ESCA model AXIS 165). Surface morphology of the samples was investigated by scanning electron microscopy (SEM, Jeol Model JSM-6390LV Microscope). UV-vis. optical transmission spectra of the samples were recorded using spectrophotometer (JASCO V-550). Photoluminescence spectra of the samples were recorded using a spectroflourometer (Perkin Elmer LS 55) equipped with a 40 W Xenon lamp. Excitation wavelength used was 320 nm. The dc electrical resistivities of the samples are studied using 617-programmable electrometer in association with Lakeshore temperature controller at room temperature.

III. RESULTS AND DISCUSSION

A. XRD studies

Figure 1 shows the XRD patterns of pure and Ni doped ZnO thin films annealed at 573 K. Undoped and doped films have a polycrystalline hexagonal wurtzite structure. With increase in Ni doping concentration, the full width at half maximum (FWHM) of the characteristic ZnO (002) peak decreases. This indicates that Ni ions can inhibit the aggregation of ZnO nanocrystals and affect the crystallization of ZnO. Structural parameters of the investigated films are given in table 1. Variation of average crystallite size with increase in Ni content in films is shown in fig. 2. The average crystallite size, calculated using Debye-Scherrer equation [17] was found to increase with increase in Ni content. This may be because presence of Ni content in concentrations used in the present study has helped in stabilizing the sol. In the film 0.5NZO, (200) plane of NiO is observed, which indicates the possibility of phase separation at this doping level. Formation of NiO secondary phase may be because Ni content has exceeded the solubility limit of Ni in ZnO matrix [18].

Dislocation density (δ) which represents the amount of defects in the crystal was estimated using the relation [19],

$$\delta = 1/D^2 \qquad (1)$$

was found to decrease with increase in Ni content.

Lattice parameter ‘c’ of the films is calculated [19] and is given in table 1. Value of ‘c’ is significant as it gives an indication of strain in the films along the ‘c’ direction (ε_1). If ‘c’ values are greater than that of the bulk (0.5206 nm), the films posses tensile or positive strain. But if ‘c’ values are smaller than that of the bulk, then the films posses compressive or negative strain. Pure, 0.1, 0.2 and 0.3 at% Ni doped ZnO thin films exhibit tensile strain, whereas 0.4 and 0.5 at% Ni doped films exhibit compressive strain. Strain in the plane of the film (ε_2) is calculated and is given in table 1.

For the films ZO, 0.1NZO, 0.2NZO and 0.3NZO, 2θ values are smaller than that of the bulk, indicating compressive stress in these films. But for the films 0.4NZO and 0.5NZO, 2θ values are higher than that of the bulk, indicating that the films are in a state of tensile stress [20]. Change in stress can be attributed to various factors. Stress is primarily due to defects produced during the growth process. During film deposition, Zn atoms occupy octahedral Zn interstitials. Simultaneously, oxygen atoms have a tendency to deviate from their positions in the ZnO crystal lattice, contributing to a large number of oxygen vacancies in the films. Gupta et al has attributed change in stress due to interstitial oxygen [21]. But, Liu et al has attributed it to oxygen vacancies and interstitial Zn atoms [22]. If interstitial Zn atoms and Zn atoms at the normal sites exclude each other, it leads to an expansion of the film lattice. But the existence of oxygen vacancies destroys the balance of attraction and repulsion between neighboring crystal planes, which leads to the contraction of film lattice.

Lattice deviation of Ni doped films from that of stress-free Zn bulk powder can cause the formation of oxygen vacancies and interstitial Zn. These defects contribute to the PL emission that is discussed later in text.

Value of lattice parameter ‘c’ approaches the value of bulk ZnO in the film 0.3NZO. Lattice strain and stress is least for this film. Hence doping concentration of 0.3 at% can be chosen as the optimum Ni doping concentration for obtaining Ni doped ZnO films with better structural properties.

B. SEM analysis

Figure 3 shows the surface SEM images of the Ni doped ZnO thin films 0.1NZO, 0.3NZO and 0.5NZO. The films were crack-free and had good adherence to the substrate used. Surface morphology of the films is modified significantly when doped with Ni. Clear hexagonal shaped granules of varying grain sizes can be observed on the surface of the film 0.5NZO.

Fig.1: XRD patterns of pure and Ni doped ZnO thin films

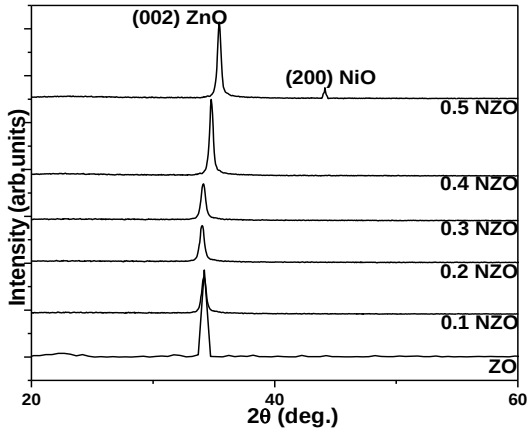

Fig.2: Variation of average crystallite size with Ni doping concentration

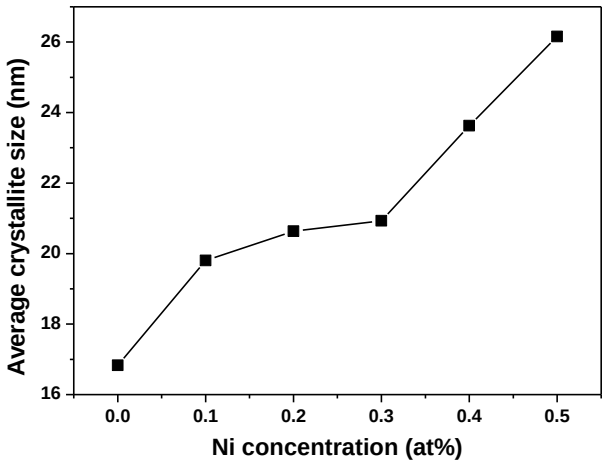

C. XPS studies

Chemical state of Ni in a representative film, 0.3NZO was analysed using XPS spectra. The survey spectrum is shown in fig. 4(a). All the spectra are corrected with respect to the standard peak of C 1s at 284.6 eV. Peak position depends on the local structure of the atoms, which indicates the chemical state of the element. The Zn 2p spectra consist of a doublet: Zn $2p_{1/2}$ and Zn $2p_{3/}$ at 1042.51 and 1022.59 eV respectively. These binding energy values closely matches with the standard values of ZnO [23] suggesting that Zn exists in +2 oxidation state. Broad and asymmetric nature of O 1s spectra can be attributed to the various coordination of oxygen in the films [8, 24]. Binding energy peak at 530.4 eV is attributed to O^{2-} ions in wurtzite structure of hexagonal Zn^{2+} ion array.

Binding energy peak at 852.90 eV is the characteristic of metallic Ni $2p_{3/2}$ state. The satellite peak at 859.32 eV in the spectrum reveals that Ni atoms are present in oxygen environment [20]. Binding energy peak at 869.18 eV closely matches with the reported value of NiO [25] indicating that Ni is present in +2 oxidation state. The energy difference between the two peaks is 16.28 eV which is strikingly different from that of NiO indicating that Ni has substituted Zn in the lattice, instead of forming any secondary phase. Thus, XPS spectra suggest that Ni atoms in the film can have mixed oxidation state of 0 and +2. It is expected that Ni^{2+} has been effectively doped into the ZnO wurtzite lattice at the Zn^{2+} sites, while metallic Ni exists in the interstices of ZnO wurtzite lattice or at the grain boundaries of the ZnO matrix [20].

D. Optical studies

Fig. 5 shows the optical transmittance spectra of pure and Ni doped ZnO thin films deposited on glass substrates. Average transmittance of 70% in the visible region is obtained in all the films. The absorption edge was found to exhibit a blue shift indicating an increase in band gap with increase in Ni doping concentration. This blue shift of absorption edge may be the result of doping-induced film degradation [26]. From the transmittance spectra absorption coefficient was evaluated using the following relation [27],

$$T = \exp(-\alpha t) \quad (2)$$

where t is the film thickness, α, the absorption coefficient and T, the transmittance of the film. The thickness and refractive index (n) of the films were evaluated using the method suggested by Sreemany et al [28] and is given in table 2. Porosity (P) of the films were calculated using the relation

$$P = 1 - [(n^2 - 1) / (n_b^2 + 1)] \quad (3)$$

where n_b is the refractive index of the bulk ZnO (n_b=2). Decrease in porosity accompanied by an increase in refractive index is observed with increase in Ni content. The optical band gap E_g was estimated using the Tauc plot [27] following the relation,

$$\alpha h\nu = A(h\nu - E_g)^n \quad (4)$$

where A is a constant, ν, the transition frequency and the exponent 'n' characterizes the nature of band transition. n=1/2 and 3/2 corresponds to direct allowed and direct forbidden transitions and n=2 and 3 corresponds to indirect allowed and indirect forbidden transitions respectively. Optical band gap can be obtained from extrapolation of the straight line portion of the $(\alpha h\nu)^2$ vs. hν plot to the position hν=0.

Optical band gap of the films was found to increase with increase in Ni content. Optical band gap of NiO is 4.0 eV, which is higher than that of bulk ZnO (3.3 eV). Hence optical band gap of Ni doped ZnO films should be higher than that of bulk ZnO. Similar observations for increase in optical band gap with increase in Ni content have been reported in literature [6, 7, 18]. The increase in optical band gap can be attributed to the sp – d spin exchange interaction between the band electrons and localised spin of the transition metal ions [29].

Table 1: Structural parameters of pure and Ni doped ZnO thin films

Sample	2θ (deg)	D(nm)	δ (x10^{-3}) (nm^{-3})	c (nm)	ε_1	σ (GPa)
ZO	34.22	16.83	3.53	0.5234	0.5378	1.2532
0.1NZO	34.03	19.80	2.55	0.5262	1.0757	2.5063
0.2NZO	34.14	20.63	2.34	0.5247	0.7683	1.8350
0.3NZO	34.18	20.93	2.28	0.5240	0.6531	1.5217
0.4NZO	34.79	23.63	1.79	0.5150	-1.0757	-2.5063
0.5NZO	35.44	26.16	1.46	0.5059	-2.8428	-6.5791

Table 2: Optical parameters of pure and Ni doped ZnO thin films

Sample	E_g (eV)	t (nm)	n	P(%)
ZO	3.21	288.16	1.81	24.13
0.1NZO	3.28	330.69	1.83	21.70
0.2NZO	3.29	347.62	1.81	24.13
0.3NZO	3.41	259.98	1.93	9.17
0.4NZO	3.39	314.61	1.95	6.58
0.5NZO	3.44	235.76	1.98	2.65

Fig.3: SEM images of (a) 0.1 (b) 0.3 (c) 0.5 at% Ni doped ZnO thin films

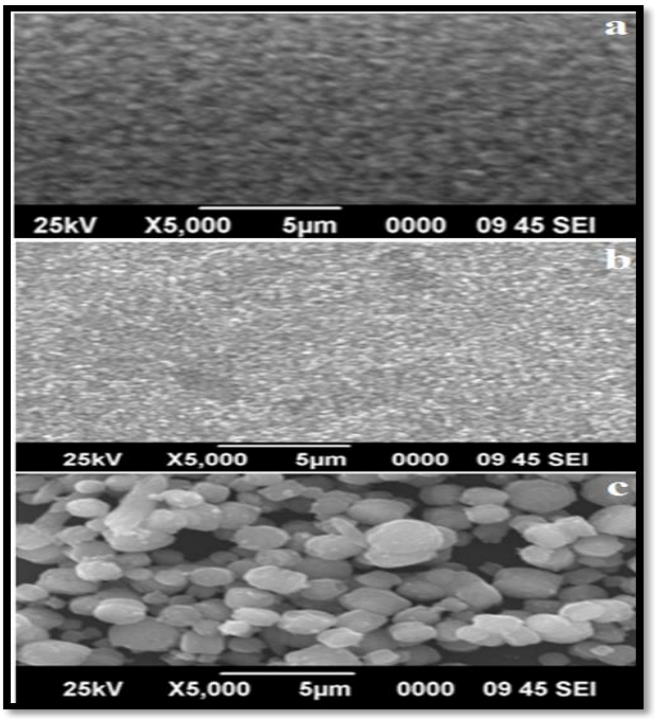

Fig.4: XPS spectrum of 0.3 at% Ni doped ZnO thin film

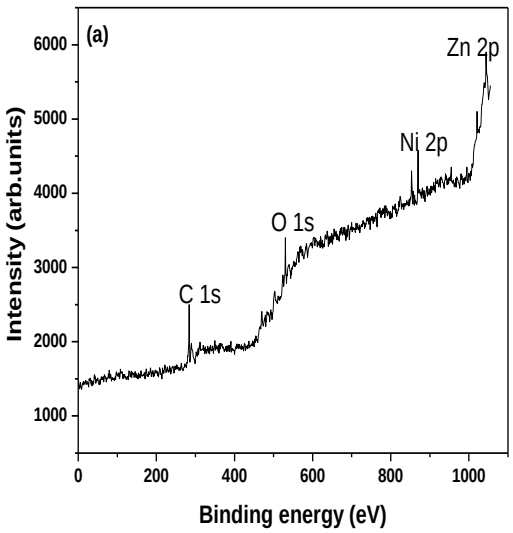

Fig.5: UV-vis Optical transmission spectra of (a) pure (b) 0.1 (c) 0.2 (d) 0.3 (e) 0.4 (f) 0.5 at% Ni doped ZnO thin films.

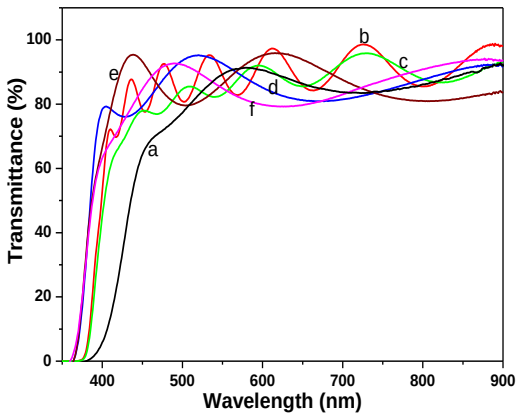

Fig.6 : Photoluminescence spectra of (a) pure (b) 0.1 (c) 0.3 (d) 0.5 Ni doped ZnO thin films

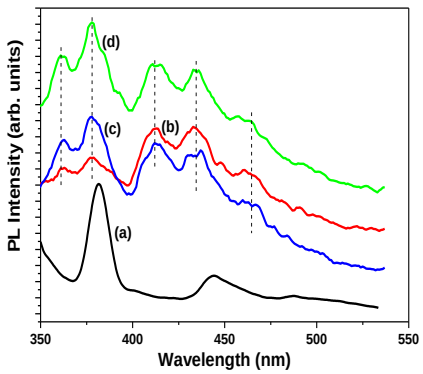

Fig.7: Variation of resistivity with Ni doping concentration

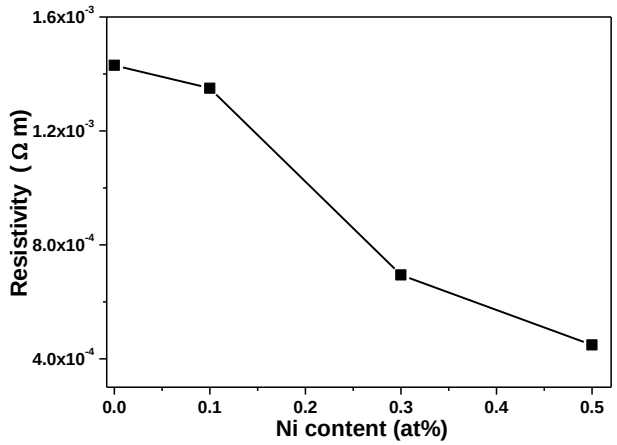

E. Photoluminescence studies

It is well known that, at room temperature ZnO can typically exhibit both UV and visible emissions. UV emission can occur due to two reasons (a) band to band transition (b) excitonic combination. The energy of band to band transition is equal to or higher than the band gap of ZnO. The energy of excitonic combination is less than the band gap of ZnO. Visible emissions are due to intrinsic defects. Six intrinsic defects are observed for ZnO (a) oxygen vacancy (b) Zn vacancy (c) oxygen atom in the position of Zn atom in the crystal lattice (d) Zn atom in the position of oxygen atom in the crystal lattice (e) oxygen interstitial (f) Zn interstitial [1].

Figure 6 shows the photoluminescence emission spectra of the films ZO, 0.1NZO, 0.3NZO and 0.5NZO respectively. Pure ZnO films possess a strong UV emission peak at 381.58 nm due to excitonic combinations [30] and a weak defect related emission at 443.76 nm due to interstitial zinc vacancy [31]. UV emission was observed at 378.82 nm in all Ni doped films. This blue shift of UV emission when doped with Ni, can be correlated with the blue shift in absorption edge observed in the optical transmittance spectra. The peak at 361.36 nm observed in all Ni doped films corresponds to the absorption of the mixture of both free excitons and free carriers. It is known that excitons in ZnO materials have large binding every (60 meV), compared to the average thermal energy (26 meV) at room temperature. Thus even at room temperature, exciton absorption plays an important role in optical transitions. [32].

Three lobes centered around 412.10, 434.42 and 464.58 nm related to defect level emission is observed in all Ni doped films. The peak at 412.10 nm is related to the interface traps existing in the depletion regions between the ZnO–ZnO grain boundaries [33,34]. The peak at 434.42 nm may be attributed to interstitial zinc vacancy [30]. Wang et al [35] has reported that Zn vacancies can lead to the spin polarisation of O 2p orbitals resulting in magnetic behaviour of ZnO materials. It is expected that the presence of PL peak in Ni doped ZnO thin films due to emission from Zn vacancies can result in magnetic behaviour of the films. The peak at 464.58 nm (2.7 eV) is related to transition of electrons from the shallow donor levels created by oxygen vacancies in the film to the valence band [1, 19].

F. Electril studies

Figure 7 show the variation in resistivity of Ni doped ZnO thin films. Resistivity of pure ZnO thin film is $1.43x10^{-3}$ Ωm. The films 0.1NZO, 0.3NZO and 0.5NZO showed a resistivity of $1.35x10^{-3}$, $6.94x10^{-4}$ and $4.48x10^{-4}$ Ωm respectively. Thus a decrease in film resistivity was observed with Ni doping. XRD analysis indicate that the average crystallite size of the films increase with Ni doping. SEM images also indicate an increase in grain size with increase in Ni content. Larger grain size causes a decrease in grain boundary. This results in decrease in oxygen adsorption at the grain boundaries, which leads to a reduction in carrier trapping within the films. This leads to a decrease in resistivity of the Ni doped films [18, 36]

IV. CONCLUSION

Pure and Ni doped ZnO thin films were deposited onto glass substrates by sol-gel spin coating technique. Structural, compositional, morphological, optical, luminescence and electrical properties of the films were investigated to explore the influence of Ni dopant concentration on ZnO thin films. XRD analysis shows an increase in average crystallite size with increase in Ni content. At lower Ni doping concentrations the films were in a state of compressive stress, but at higher Ni concentration of 0.4 and 0.5 at% the films were in a state of tensile stress. XPS studies on 0.3at% Ni doped ZnO films showed that Ni atoms were present in mixed oxidation state of 0 and +2. Optical band gap was found to increase from 3.21 to 3.44 with increase in Ni content from 0 to 0.5 at% which is attributed to the sp – d spin exchange interaction between the band electrons and localised spin of the transition metal ions. An increase in refractive index from 1.81 to 1.98 was observed with increase in Ni content. Photoluminescence spectra featured emissions in both UV and visible region in all the investigated samples. Resistivity of the films was found to decrease with increase in Ni content.

REFERENCES

1. Zhaoyang W, Lizhong H (2009) Vacuum 83:906
2. Aly S.A, Sayed N. Z. El, Kaid M.A (2001) Vacuum 61:1
3. Bachari E.M, Baud G, Ben A.S, Jacquet M(1999) Thin solid Films 348:165
4. Krunks.M, Mellikov E (1995) Thin Solid Films 270:33
5. Olvera M.L, Maldonado A, Asomaza R, Asomoza M (1993) Thin solid Films 229:196
6. Farag A.A.M, Cavas M, Yakuphanoglu F, Amanullah F.M (2011) J. Alloys Compd. 509: 7900
7. Yan X, Hu D, Li H, Chong X, Wang Y (2011) Physica B 406: 3956
8. Pandey B, Ghosh S, Srivastava P, Kabiraj D, Shripati T, Lalla N.P (2009) Physica E 41: 1164

9. Liu E, Xiao P, Chen J.S, Lim B.C, Li L (2008) Current Appl. Phys. 8:408
10. Sahu D.R (2007) Microelectron.J. 38:1252
11. Makino T, Isoya G , Segawa Y, Chia C.H, yasuda T, Kawasaki M, ohtomo A, Tamura K, koinuma H (2000) J.Crystal Grwoth, 289:214
12. Park S.J, Jang S.J, Kim S.S, Lee B.T (2006) Appl.Phys.Lett. 89:121108
13. King S.L, Gardeniers J.G.E, Boyd I.W (1996) Appl.Surf.Sci. 811:96
14. Mridha S, Basak D (2007) Mater.Res.Bull. 42:875
15. Lin K.M, Tsai P (2007) Thin Solid Films 515:8601
16. Kamalasanan M.N, Chandra S (1996) Thin Solid Films 228:112
17. Cullity B.D (1978) Elements of X-ray diffraction (Addison-Wesley Reading)
18. Kim K, Kim G, Woo J. Kim C (2008) Surf. Coat. Tech. 202: 5650
19. Santhosh V S, Babu K R, Deepa M (2014) J Mater. Sci. Mater. Electron 25: 224
20. Zhao X, Liu E, Ramanujan R.V, Chen J (2012) Curr. Appl. Phys. 12: 834
21. Gupta V, Mansingh A (1996) J. Appl.Phys. 80: 1063
22. Liu X.J, Song C, Zeng F, Wang X.B, Pan F (2007) J.Phys. D: Appl. Phys. 40: 1608
23. U Ilyas, R. S. Rawat, T.L.Tan, P.Lee, R.Chen, J.Appl.Phys. 111 (2012) 033503
24. Chen M, Wang X, Yu Y.H, Pei Z.L, Bai X.D, Sun C, Huang R.F, Wen L.S (2000) Appl.Surf. Sci. 158:134
25. Wagner C.D, Riggs W.M, Davis L.E, Moulder J.F, Muilenberg G.E (1979) Handbook of X-ray photoelectron spectroscopy Perkin Elemer, Eden Prairie p.80
26. Tan S.T, Chen B.J, Sun X.W, Fan W.F, Kwok H.S, Zhang X.H, Chua S.J (2005) J.Appl.Phys. 98: 013505
27. Tauc J, Grigorovici R, Vancu A (1966) Phys. Status Solidi. 15: 627
28. Sreemany M, Sen S (2004) Mater. Chem. Phys. 83:169
29. Mandal S.K, Nath T.K (2006) Thin Solid Films 515: 2535
30. Kurbanov S.S, Panin G.N, Kim T.W, Kang T.W (2008) Phys. Rev. B 78: 045311
31. Xu P.S, Sun Y.M, Shi C.S, Xu F.Q, Pan H.B (2003) Nucl.Instrum.Meth.In Phys. Res. B 199:286
32. Shi W.S, Agyeman O, .Xu C.N (2002) J.Appl.Phys. 9:15640
33. Jin B.J, Woo H.S, Im S, Bae S.H, Lee S.Y (2001) Appl. Surf. Sci. 169:521
34. Fan D.H, Ning Z.Y, Jiang M.F (2005) Appl.Surf.Sci. 245:414
35. Wang Q, Sun Q, Chen G, Kawazoe Y, Jena P (2008) Phys. Rev. B 77: 205411
36. Malek M F, Mamat M H, Sahdan M Z, Zahidi M M, Khusaimi Z, Mahmood M R (2013) Thin Solid Films 527: 102